

Evaluation of a Non-Coherent Ultra-Wideband Transceiver for Micropower Sensor Nodes

Jonah Imfeld , Silvano Cortesi , Philipp Mayer , Michele Magno 

Dept. of Information Technology and Electrical Engineering, ETH Zürich, Zürich, Switzerland

Abstract— Spatial and contextual awareness has the potential to revolutionize sensor nodes, enabling spatially augmented data collection and location-based services. With its high bandwidth, superior energy efficiency, and precise time-of-flight measurements, ultra-wideband (UWB) technology emerges as an ideal solution for such devices.

This paper presents an evaluation and comparison of a non-coherent UWB transceiver within the context of highly energy-constrained wireless sensing nodes and pervasive Internet of Things (IoT) devices. Experimental results highlight the unique properties of UWB transceivers, showcasing efficient data transfer ranging from 2 kbit/s to 7.2 Mbit/s while reaching an energy consumption of 0.29 nJ/bit and 1.39 nJ/bit for transmitting and receiving, respectively. Notably, a ranging accuracy of up to ± 25 cm can be achieved. Moreover, the peak power consumption of the UWB transceiver is with 6.7 mW in TX and 23 mW in RX significantly lower than that of other commercial UWB transceivers.

Index Terms—Wireless communication, ultra-wideband (UWB), Internet of Things (IoT), localization, ultra-low power, sensor systems and applications.

I. INTRODUCTION

The increasing adoption of Internet of Things (IoT) sensors and devices has sparked a demand for pervasive location services. In addition to prominent applications such as navigation and asset tracking, the inclusion of location awareness in sensors has the intriguing ability to expand the horizons of mobile IoT systems[1], [2]. It empowers them to interact with the surrounding environment and potentially paves the way for contextual understanding, opening new possibilities for innovation and sensor interaction [3]–[5].

While accurate outdoor localization is achievable using the global navigation satellite system (GNSS), indoor and hybrid scenarios lack widely adopted solutions. Indoor location services present a larger market potential, thus driving research efforts toward GNSS-like indoor localization technologies [6].

Ultra-wideband (UWB) based on IEEE 802.15.4z has emerged as a leading choice for high-accuracy device-based indoor localization [7]. With its sub-nanosecond pulses and the resulting superior time resolution, UWB enables precise time-of-flight (ToF) measurements [8], allowing for accurate distance estimation and ranging. Alongside the ranging capabilities, UWB has the potential for highly energy-efficient communication, particularly on the transmitter side and when utilizing non-coherent receiver implementations, making it a promising technology for battery- or energy-harvesting powered devices [9]–[11].

One significant drawback of commercial UWB transceivers is their high peak power consumption, which presents challenges for small-sized battery-powered devices. In addition, it is crucial to eliminate the need for periodic synchronization between these devices and infrastructure and to achieve near zero watts idle consumption to enable long-term operation without frequent recharging or replacement [4]. To incorporate the ability of accurate ranging and efficient communication in a single device, a hybrid wireless frontend is often implemented that uses both Bluetooth Low Energy (BLE) and UWB [12], [13].

This work comprehensively and accurately evaluates the SPARK MICROSYSTEMS SR1000 series, a promising ultra-wideband transceiver that combines key features suitable for highly energy-constrained systems. In particular, the main contributions of this work are as follows: *(i)* A comprehensive analysis of the energy consumption and the optimal configuration to balance data rate and power consumption; *(ii)* An accurate survey on recently released commercial UWB transceivers; *(iii)* An evaluation of the ranging capability, demonstrating a ranging accuracy of up to ± 25 cm.

The rest of the paper is organized as follows: Section II presents the recent literature and discusses key performance indicators of commercial UWB transceivers; Section III introduces the experimental setup; Section IV shows experimental results and possible applications; Finally, section V concludes the paper.

II. RELATED WORK

In addition to UWB, BLE stands out as one of the most widely adopted technologies for low-power data transmission and positioning. With the standardization of BLE direction finding and its availability in modern and low-cost system-on-chips (SoCs) such as the nRF5340, BLE showed itself effective for localization through angle of arrival (AoA) and multi-carrier phase-difference (MCPD) [14]. Depending on the filters used, the ranging accuracy is below 60 cm [15], [16], while an AoA accuracy of 10° can be achieved at 5 m [17]. The power consumption of BLE makes it particularly suited for micropower sensors, demonstrating 11.2 mW and 9.5 mW for TX and RX, respectively, with a data rate of 2 Mbit/s [18]. An overview of the state-of-the-art commercial UWB transceivers and their comparison against BLE is given in Table I.

In [13], Coppens et al. give an overview of the current state of UWB modules and standards. The IEEE 802.15.4z standard is supported by all popular integrated circuits (ICs)

TABLE I: Comparison of common UWB and BLE radio system-on-chips.

	nRF5x BLE [15]–[18]	Qorvo DW3220 [19], [20], [23]	NXP SR040, SR150 [21], [22], [24]	Microchip ATA8352 [8], [25], [26]	Spark SR1000 [27], [28]
Frequency range [GHz]	2.4	6-8.5	6.2-8.2	6.2-8.3	SR1010: 3.1-5.8, SR1020: 6-9.3
3dB Bandwidth [GHz]	-	0.5	0.5	0.5	3
Max. Data rate [Mbps]	2	6.8	31.2	1	10
Ranging / AoA Type	RSSI, MCPD, I/Q	TWR, TDoA, PDoA	TWR, TDoA, (PDoA)	TWR, TDoA	TWR
Ranging Accuracy [cm]	± 60	± 5	± 10	± 5	± 30
AoA Accuracy [$^{\circ}$]	± 10	± 5	± 3	-	-
Shutdown Power draw [nW]	1620	468	900	87	181
Peak TX Power draw [mW]	11.2	63	236	30	SR1010: 6.7 , SR1020: 6.3
Peak RX Power draw [mW]	9.5	158	207	130	SR1010: 23 , SR1020: 21.2
IEEE802.15.4z Compliance	-	✓	✓	✓	✗
UWB PHY Type	-	HRP	HRP	LRP	Custom
Supported Channels	-	5 & 9	5, 6, 8 & 9	-	-
FirA Cerification	-	✓	✓	✗	✗

except the SR1000, as shown in Table I. The devices based on IEEE 802.15.4z can be split into those supporting high-rate pulse repetition (HRP) (QORVO DW3xxx, NXP SR040 & SR150) and those supporting low-rate pulse repetition (LRP) (MICROCHIP ATA8352). As shown in [19], [20], the DW3x20 devices achieve an accuracy of 5° for AoA and below 5 cm at a power consumption of 55 mW. [21], [22] characterized the NXP SR040 and SR150 and found its accuracy to be below 8° or 15 cm. An evaluation of Flueratoru et al. [8] showed that the 3DB ACCESS 3DB6830C, the predecessor of the MICROCHIP ATA8352, achieved a similar ranging accuracy of up to 5 cm in line-of-sight (LOS) conditions. The power consumption of the 3DB6830C is 20.7 mW during TX and 40.7 mW during RX. The increased energy efficiency of LRP-based devices comes at the cost of a limited data rate of max. 10 Mbit/s [13]. The SR1000 places itself in between LRP and HRP, with the purpose of attaining both low power consumption and high throughput.

III. MEASUREMENT SETUP

The SR1000 evaluation kit (EVK) from SPARK MICROSYSTEMS is used as a platform to carry out all the measurements. It includes an STM32G473 microcontroller (MCU), a lipo battery with a charging circuit, and interchangeable transceiver modules. The transceiver modules include the SR1010 or SR1020 transceiver and a monopole printed circuit board (PCB) microstrip antenna. The specific modules used are the RMV8QMREV150 for the SR1010 and the RMV8QEUMMREV120 for the SR1020. Power measurements were conducted using a KEYSIGHT N6781A power analyzer connected to the module's current measurement header that is directly connected to the transceiver IC. Along with the EVK, an application binary controllable by a graphical user interface (GUI) is provided by SPARK.

IV. EXPERIMENTAL RESULTS

A. Power Consumption with Experimental Measurements

Firstly, the static power consumption is analyzed. The transceivers allow five static configurations: shutdown mode, deep and shallow sleep, idle, or receiving. For each state, the current was measured at 1.8 V and 3.3 V by substituting the

board supply with a source measurement unit. Deeper power states result in lower idle consumption but at the cost of higher wake-up time and energy.

The results of the static power consumption measurements are summarized in Table II. It should be noted that the startup cost from the shutdown state is around $500 \mu\text{J}$ at 1.8 V due to the need to recalibrate the transceiver for 20 ms. Consequently, entering the shutdown state becomes advantageous only if no message exchanges occur for a minimum period of 644 s for the SR1010 IC at 1.8 V.

Secondly, the transmission and reception power consumption is measured in a data streaming configuration at 1.8 V. The devices are set to transmit random data with on-off keying (OOK) modulation and deactivated forward error correction. Channel switching is used to maximize the link budget. The measurements are taken at an output power of 0 dBFS and -9 dBFS . The data rate has been adjusted by varying the packet rate while maintaining a fixed payload size of 124 bytes. As the minimum packet rate configurable through the GUI is 200 packets/s, the payload size below has been reduced to accommodate data rates lower than 0.198 Mbps.

The power consumption for transmission and reception in a datastream configuration is depicted in Fig. 1a) and Fig. 1b), respectively. The underlying power state is indicated within grey boxes. The relatively higher power consumption for SR1010 RX at -9 dBFS in the deep sleep state is linked to a low packet delivery ratio which causes the receiver to remain active for longer.

Due to the high start-up energy cost of the deep sleep state, it is found to be less efficient compared to the shallow

TABLE II: Static current consumption as a function of the power mode and supply voltage.

Transceiver	SR1010		SR1020	
	1.8 V	3.3 V	1.8 V	3.3 V
Shutdown	44 nA	100 nA	39 nA	104 nA
Deep Sleep	475 nA	819 nA	466 nA	844 nA
Shallow Sleep	39.1 μA	40.0 μA	39.5 μA	40.5 μA
Idle	351.9 μA	263.6 μA	380.6 μA	269.2 μA
Active RX	11.5 mA	7.2 mA	12.7 mA	7.7 mA

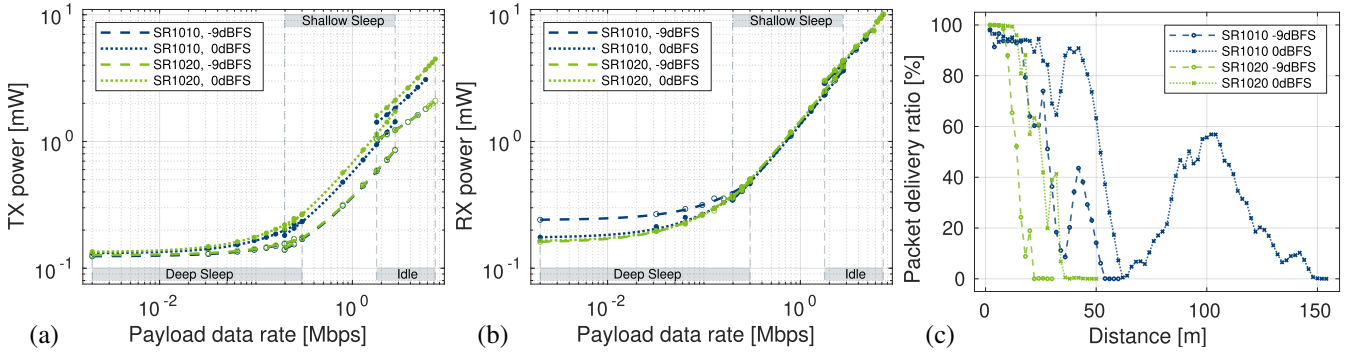


Fig. 1: Power consumption during (a) TX and (b) RX data streaming. (c) Packet delivery ratio of the SR1000 SoCs.

sleep state, even at the lowest packet rate of 200 packets/s. With SR1010, a stable connection could be maintained up to 5.75 Mbps, while with SR1020, the stable connection extended up to 7.24 Mbps. At a data rate of 1.29 Mbps, which is close to the theoretical payload data rate limit of BLE 5 [29], SR1000 consumes as little as 0.45 mW or 0.35 nJ/bit while transmitting and 1.73 mW or 1.34 nJ/bit during reception.

B. Communication Range

To assess the maximum usable range, two EVKs are placed facing each other in an open field at a height of 1.5 m. One device has been configured to operate as a transmitter, sending a one-byte payload with 2bit-pulse-position modulation (2bit-PPM) at a rate of 1000 packets/s. The transmitter counts the number of packets that are successfully acknowledged by the receiving node and calculates the packet delivery ratio (PDR) over 10 k transmissions based on Eq. (1). After each measurement, the distance between the two nodes has been increased by 2 m.

$$PDR = \frac{\# \text{ ACKNOWLEDGED PACKETS}}{\# \text{ SENT PACKETS}} \quad (1)$$

In Fig. 1c), the measured PDR for both devices is shown at the two output power settings employed during the power consumption measurements. The SR1010 PDR exhibits a significant drop in PDR at 30 m and 60 m, followed by a subsequent recovery. This pattern has been observed consistently at three separate measurements. It is most likely caused by

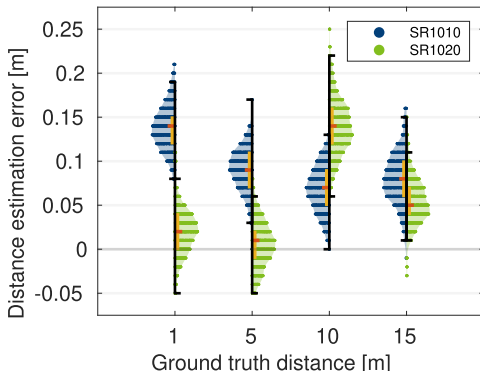


Fig. 2: Ranging accuracy for different ground truth distances and the two evaluated UWB ICs.

multipath reflections, as other measurements with the nodes at the height of 1 m and 2.5 m yielded different results.

C. Time-of-Flight Ranging

To analyze the ranging capabilities, the GUI's ranging example is used in the high output power and high precision configuration. The nodes are set up similarly to section IV-B but at a distance of 1, 5, 10, and 15 m apart from each other. The precise distance between the nodes has been determined using a LEICA DISTO X310, which served as the ground truth distance. At each distance, 1 k samples have been collected. Prior to the measurement, the transceivers are calibrated according to the application note by SPARK.

Fig. 2 presents the distribution of the measured distance estimation error. The mean error is indicated in orange, while the 50 % error window is highlighted in yellow. Using the SR1010 transceiver, ranging is achievable up to a distance of 52 m, with SR1020 up to 32 m. The high output power setting in the GUI corresponds to -5.4 dBFS, which aligns well with the range data measured in Section IV-B.

V. CONCLUSION

This paper presented an analysis of the SPARK MICROSYSTEMS SR1000 family in the context of low-power, spatial-aware IoT applications. This includes a comparison to the most popular UWB ICs and BLE. Experimental evaluations have shown the capabilities of the SR1000 to achieve a high throughput of up to 7.24 Mbit/s with a very high bit efficiency of 0.29 nJ/bit when transmitting and 1.39 nJ/bit while receiving. In particular, it proves to be a real alternative to BLE: At a data rate of 2 Mbit/s, the bit energy efficiency is about 5× higher than BLE, especially for the transmitter at 0.6 nJ/bit compared to BLE's 5.6 nJ/bit. With a ranging accuracy of ± 25 cm, SR1000 is up to 2× better than BLE, but it falls behind state-of-the-art UWB ICs which can reach an accuracy of ± 5 cm. The results show the transceiver's potential to perform well in a wide range of applications due to its low power demand over a wide range of data rates and the ability to perform accurate ranging measurements.

ACKNOWLEDGMENTS

The authors would like to thank armasuisse Science & Technology for funding this research.

REFERENCES

- [1] D. Zou, W. Meng, S. Han, K. He, and Z. Zhang, "Toward Ubiquitous LBS: Multi-Radio Localization and Seamless Positioning," *IEEE Wireless Communications*, vol. 23, no. 6, pp. 107–113, 2016, doi: 10.1109/MWC.2016.1500177WC.
- [2] Y. Li *et al.*, "Toward Location-Enabled IoT (LE-IoT): IoT Positioning Techniques, Error Sources, and Error Mitigation," *IEEE Internet of Things Journal*, vol. 8, no. 6, pp. 4035–4062, 2021, doi: 10.1109/JIOT.2020.3019199.
- [3] A. Elsharkawy, K. Naheem, D. Koo, and M. S. Kim, "A UWB-Driven Self-Actuated Projector Platform for Interactive Augmented Reality Applications," *Applied Sciences*, vol. 11, no. 6, 2021, doi: 10.3390/app11062871.
- [4] P. Mayer, M. Magno, and L. Benini, "Self-sustaining Ultra-wideband Positioning System for Event-driven Indoor Localization," *IEEE Internet of Things Journal*, pp. 1–13, 2023, doi: 10.1109/JIOT.2023.3289568.
- [5] C. Zhao, A. Song, Y. Zhu, S. Jiang, F. Liao, and Y. Du, "Data-Driven Indoor Positioning Correction for Infrastructure-Enabled Autonomous Driving Systems: A Lifelong Framework," *IEEE Transactions on Intelligent Transportation Systems*, vol. 24, no. 4, pp. 3908–3921, 2023, doi: 10.1109/TITS.2022.3233563.
- [6] M. A. Cheema, "Indoor location-based services: Challenges and opportunities," *SIGSPATIAL Special*, vol. 10, no. 2, p. 10–17, nov 2018, doi: 10.1145/3292390.3292394.
- [7] Y. Ibnatta, M. Khalid, and M. Sadik, *Exposure and Evaluation of Different Indoor Localization Systems*, ser. Proceedings of Sixth International Congress on Information and Communication Technology. Springer Singapore, 2021, pp. 731–742.
- [8] L. Fluerautoru, S. Wehrli, M. Magno, E. S. Lohan, and D. Niculescu, "High-accuracy ranging and localization with ultrawideband communications for energy-constrained devices," *IEEE Internet of Things Journal*, vol. 9, no. 10, pp. 7463–7480, 2022, doi: 10.1109/jiot.2021.3125256.
- [9] D. Dardari *et al.*, "An Ultra-Low Power Ultra-Wide Bandwidth Positioning System," *IEEE Journal of Radio Frequency Identification*, vol. 4, no. 4, pp. 353–364, 2020, doi: 10.1109/JRFID.2020.3008200.
- [10] J. Bauwens, N. Macoir, S. Giannoulis, I. Moerman, and E. De Poorter, "UWB-MAC: MAC protocol for UWB localization using ultra-low power anchor nodes," *Ad Hoc Networks*, vol. 123, p. 102637, dec 2021, doi: 10.1016/j.adhoc.2021.102637.
- [11] W. S. Jeon, H. S. Oh, and D. G. Jeong, "Decision of Ranging Interval for IEEE 802.15.4z UWB Ranging Devices," *IEEE Internet of Things Journal*, vol. 8, no. 20, pp. 15 628–15 638, 2021, doi: 10.1109/JIOT.2021.3074571.
- [12] J. Kolakowski, V. Djaja-Josko, M. Kolakowski, and K. Broczek, "UWB/BLE Tracking System for Elderly People Monitoring," *Sensors*, vol. 20, no. 6, p. 1574, 2020, doi: 10.3390/s20061574.
- [13] D. Coppens, A. Shahid, S. Lemey, B. Van Herbruggen, C. Marshall, and E. De Poorter, "An Overview of UWB Standards and Organizations (IEEE 802.15.4, FiRa, Apple): Interoperability Aspects and Future Research Directions," *IEEE Access*, vol. 10, pp. 70 219–70 241, 2022, doi: 10.1109/ACCESS.2022.3187410.
- [14] S. Cortesi, C. Vogt, and M. Magno, "Comparison Between an Rssi- and an Mcpd-Based Ble Indoor Localization System," *Computers*, vol. 12, no. 3, p. 59, 2023, doi: 10.3390/computers12030059.
- [15] A. Mackey, P. Spachos, L. Song, and K. N. Plataniotis, "Improving Ble Beacon Proximity Estimation Accuracy Through Bayesian Filtering," *IEEE Internet of Things Journal*, vol. 7, no. 4, pp. 3160–3169, 2020, doi: 10.1109/jiot.2020.2965583.
- [16] X. Zhu, M. Handte, and R. Eskicioglu, "RF Technologies for Indoor Localization and Positioning," in *Proceedings of the 16th ACM Conference on Embedded Networked Sensor Systems*, 11 2018, doi: 10.1145/3274783.3275217.
- [17] F. Långberg and J. Thurborg, "Design of a size reduced antenna array for angle of arrival (aoa) estimation for ble 5.1," Master's thesis, Lund University, Department of Electrical and Information Technology, 11 2020, accessed 27.06.2023. [Online]. Available: <https://lup.lub.lu.se/luur/download?func=downloadFile&recordId=903\1557&fileId=9031558>.
- [18] Nordic Semiconductor, "nrf5340 datasheet," 2023, accessed 27.06.2023. [Online]. Available: https://infocenter.nordicsemi.com/pdf/nRF5340_PS_v1.3.pdf.
- [19] T. Margiani, S. Cortesi, M. Keller, C. Vogt, T. Polonelli, and M. Magno, "Angle of Arrival and Centimeter Distance Estimation on a Smart Uwb Sensor Node," *IEEE Transactions on Instrumentation and Measurement*, vol. 72, pp. 1–10, 2023, doi: 10.1109/tim.2023.3282289.
- [20] T. Polonelli, S. Schlapfer, and M. Magno, "Performance Comparison between Decawave DW1000 and DW3000 in low-power double side ranging applications," in *2022 IEEE Sensors Applications Symposium (SAS)*, 8 2022, doi: 10.1109/sas54819.2022.9881375.
- [21] R. Juran, P. Mlynák, M. Stusek, P. Masek, M. Mikulásek, and A. Ometov, "Hands-On Experience with UWB: Angle of Arrival Accuracy Evaluation in Channel 9," in *2022 14th International Congress on Ultra Modern Telecommunications and Control Systems and Workshops (ICUMT)*, 10 2022, pp. 45–49, doi: 10.1109/icumt57764.2022.9943504.
- [22] A. Heinrich, S. Krollmann, F. Putz, and M. Hollick, "Smartphones with UWB: Evaluating the Accuracy and Reliability of UWB Ranging," *arXiv preprint arXiv:2303.11220*, 2023, doi: 10.48550/ARXIV.2303.11220.
- [23] Qorvo, "Qorvo dw3220 datasheet," 2020, accessed 27.06.2023. [Online]. Available: <https://www.qorvo.com/products/d/da008142>.
- [24] AMO Amosense, "Amotech sr040 & sr150 datasheet," 2023, accessible after purchase.
- [25] Microchip, "Microchip ata8352 datasheet," 2021, accessed 27.06.2023, needs registration. [Online]. Available: https://t.ly/KM_Y.
- [26] ———, "Microchip data communication and ranging," 2023, accessed 30.06.2023. [Online]. Available: <https://t.ly/Gga3>.
- [27] Spark Microsystems, "Sr1010 datasheet," 2020, accessed 27.06.2023. [Online]. Available: https://www.sparkmicro.com/wp-content/uploads/2023/04/datasheet_SR1010-4.pdf.
- [28] ———, "Sr1020 datasheet," 2020, accessed 27.06.2023. [Online]. Available: https://www.sparkmicro.com/wp-content/uploads/2023/04/datasheet_SR1020-2.pdf.
- [29] M. Woolley, "Bluetooth® Core Specification Version 5.0 Feature Enhancements," 2021, accessed 24.06.2023. [Online]. Available: https://www.bluetooth.com/wp-content/uploads/2019/03/Bluetooth_5-FINAL.pdf.